Article

Nanosized (-Pt)Pd Pt(CO)(PPh) (x 7) Containing Pt-Centered Four-Shell 165-Atom Pd–Pt Core with Unprecedented Intershell Bridging Carbonyl Ligands: Comparative Analysis of Icosahedral Shell-Growth Patterns with Geometrically Related Pd(CO)(PEt) (x 60) Containing Capped Three-Shell Pd Core

Evgueni G. Mednikov, Matthew C. Jewell, and Lawrence F. Dahl

J. Am. Chem. Soc., **2007**, 129 (37), 11619-11630• DOI: 10.1021/ja073945q • Publication Date (Web): 28 August 2007

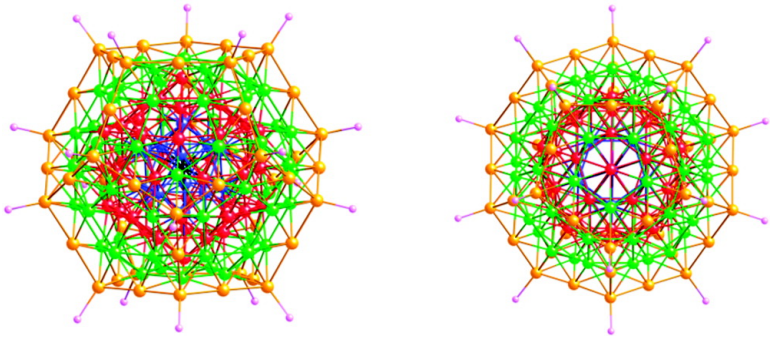

More About This Article

Additional resources and features associated with this article are available within the HTML version:

- Supporting Information
- Links to the 17 articles that cite this article, as of the time of this article download
- Access to high resolution figures
- Links to articles and content related to this article
- Copyright permission to reproduce figures and/or text from this article

View the Full Text HTML

J|A|C|S
ARTICLES
Published on Web 08/28/2007

Nanosized (μ_{12}-Pt)$Pd_{164-x}Pt_x(CO)_{72}(PPh_3)_{20}$ ($x \approx 7$) Containing Pt-Centered Four-Shell 165-Atom Pd−Pt Core with Unprecedented Intershell Bridging Carbonyl Ligands: Comparative Analysis of Icosahedral Shell-Growth Patterns with Geometrically Related $Pd_{145}(CO)_x(PEt_3)_{30}$ ($x \approx 60$) Containing Capped Three-Shell Pd_{145} Core

Evgueni G. Mednikov,*,† Matthew C. Jewell,‡ and Lawrence F. Dahl*,†

Contribution from the Department of Chemistry and Department of Materials & Engineering, University of Wisconsin-Madison, Madison, Wisconsin 53706

Received June 13, 2007; E-mail: mednikov@chem.wisc.edu; dahl@chem.wisc.edu

Abstract: Presented herein are the preparation and crystallographic/microanalytical/magnetic/spectroscopic characterization of the Pt-centered four-shell 165-atom Pd−Pt cluster, (μ_{12}-Pt)$Pd_{164-x}Pt_x(CO)_{72}(PPh_3)_{20}$ ($x \approx 7$), **1**, that replaces the geometrically related capped three-shell icosahedral Pd_{145} cluster, $Pd_{145}(CO)_x(PEt_3)_{30}$ ($x \approx 60$), **2**, as the largest crystallographically determined discrete transition metal cluster with direct metal−metal bonding. A detailed comparison of their shell-growth patterns gives rise to important stereochemical implications concerning completely unexpected structural *dissimilarities* as well as *similarities* and provides new insight concerning possible synthetic approaches for generation of multi-shell metal clusters. **1** was reproducibly prepared in small yields (<10%) from the reaction of $Pd_{10}(CO)_{12}(PPh_3)_6$ with $Pt(CO)_2(PPh_3)_2$. Its 165-atom metal-core geometry and 20 PPh_3 and 72 CO ligands were established from a low-temperature (100 K) CCD X-ray diffraction study. The well-determined crystal structure is attributed largely to **1** possessing cubic T_h ($2/m\bar{3}$) site symmetry, which is the highest crystallographic subgroup of the noncrystallographic pseudo-icosahedral I_h ($2/m\bar{3}\bar{5}$) symmetry. The "full" four-shell Pd−Pt anatomy of **1** consists of: (a) shell 1 with the centered (μ_{12}-Pt) atom encapsulated by the 12-atom icosahedral Pt_xPd_{12-x} cage, $x = 1.2(3)$; (b) shell 2 with the 42-atom ν_2 icosahedral Pt_xPd_{42-x} cage, $x = 3.5(5)$; (c) shell 3 with the *anti*-Mackay 60-atom semi-regular rhombicosidodecahedral Pt_xPd_{60-x} cage, $x = 2.2(6)$; (d) shell 4 with the 50-atom ν_2 pentagonal dodecahedral Pd_{50} cage. The total number of crystallographically estimated Pt atoms, 8 ± 3, which was obtained from least-squares (Pt_x/Pd_{1-x})-occupancy analysis of the X-ray data that conclusively revealed the central atom to be pure Pt (occupancy factor, $x = 1.00(3)$), is fortuitously in agreement with that of 7.6(7) found from an X-ray Pt/Pd microanalysis (WDS spectrometer) on three crystals of **1**. Our utilization of this site-occupancy (Pt_xPd_{1-x})-analysis for shells 1−3 originated from the microanalytical results; otherwise, the presumed metal-core composition would have been (μ_{12}-Pt)Pd_{164}. [Alternatively, the (μ_{12}-Pt)M_{164} core-geometry of **1** may be viewed as a pseudo-I_h Pt-centered *six-shell* successive ν_1 polyhedral system, each with radially equivalent vertex atoms: Pt@M_{12}(icosahedron)@M_{30}(icosidodecahedron)@M_{12}(icosahedron)@M_{60}(rhombicosidodecahedron)@M_{30}(icosidodecahedron)@M_{20}(pentagonal dodecahedron)]. Completely surprising structural *dissimilarities* between **1** and **2** are: (1) to date **1** is only reproducibly isolated as a heterometallic Pd−Pt cluster with a central Pt instead of Pd atom; (2) the 50 atoms comprising the outer fourth ν_2 pentagonal dodecahedral shell in **1** are *less* than the 60 atoms of the inner third shell in **1**, in contradistinction to shell-by-shell growth processes in all other known shell-based structures; (3) the 10 fewer PR_3 ligands in **1** necessitate larger bulky PPh_3 ligands to protect the Pd−Pt core-geometry; (4) the 72 CO ligands consist of six bridging COs within each of the 12 pentagons in shell 4 that are coordinated to *intershell* metal atoms. SQUID magnetometry measurements showed a single-crystal sample of **1** to be diamagnetic over the entire temperature range of 10−300 K.

Introduction

Our research has shown that palladium is a unique metal in its high-nuclearity homopalladium/heteropalladium cluster chemistry. Palladium forms an unparalleled homopalladium family of highly condensed CO/phosphine-ligated clusters that exhibit a remarkable geometrically unprecedented diversity of icosahedral- or ccp/hcp-based metal-core geometries that are not observed for other Group 8−10 transition metals.[1,2] To date, *nanosized* palladium carbonyl/phosphine clusters that have been isolated and crystallographically/spectroscopically character-ized

† Department of Chemistry.
‡ Department of Materials & Engineering (UW-Madison); now at Applied Superconductivity Center, Florida State University, Tallahassee, FL 32306-4390.

10.1021/ja073945q CCC: $37.00

possess 18 distinctly different Pd_n core-geometries with $n =$ 10,[3a−c] 12,[3d,e] 16,[3f,g] 23 (with two highly dissimilar metal cores),[3h−j] 29,[3e] 30,[3k] 34,[1b,3l] 35,[3g] 37,[3m] 38,[3n] 39,[3g] 52,[3o] 54,[3k] 59, [3g,p] 66,[3o] 69,[3q] and 145.[3r] All but two of their nanosized palladium cores[3n,3j] have fragments with close-packed architectures. The Pd_n cores with close-packed structural units include ones with "twinned" interpenetrating centered icosahedral and cuboctahedral geometries along with one mixed, face-fused icosahedral/octahedral Pd_{59} framework[3g] consisting of two centered icosahedra that *trans-cap* a bioctahedron. The Pd_{145} cluster[3r] differs completely from the other Pd_n clusters in possessing a concentric spheroidal-shaped *multi-shell* metal core (*vide infra*). One particularly notable property of these PR_3/CO-ligated palladium clusters is their facile lability in undergoing ligand-induced structural changes, as strikingly illustrated via the $^{31}P\{^1H\}$ NMR-monitored (PEt_3)-induced (rapid) reversible interconversion[4] between $Pd_{23}(CO)_{20}(PEt_3)_{10}$[3i] and $Pd_{23}(CO)_{20}(PEt_3)_8$,[3j] which possess highly dissimilar Pd_{23} core-geometries due to the former having two additional PEt_3 ligands.

In an ongoing systematic investigation to generate nanosized Pd−Pt carbonyl clusters by reactions of zerovalent palladium/platinum clusters, we have isolated the remarkable Pt-centered four-shell 165-atom Pd−Pt cluster, $(\mu_{12}\text{-Pt})Pd_{164-x}Pt_x(CO)_{72}(PPh_3)_{20}$ ($x \approx 7$), **1**, which is the successor of $Pd_{145}(CO)_x(PEt_3)_{30}$ ($x \approx 60$), **2**,[3r] as the largest crystallographic example of a discrete transition metal cluster with direct metal−metal bonding. This latter homopalladium **2** was initially isolated in extremely low yields via reduction of a mixture of $Pd(PEt_3)_2Cl_2$ and $Au(PPh_3)Cl$ with CO in the presence of NaOH, and its metal-core geometry was unambiguously determined from crystallographic analyses of CCD X-ray data for two crystals from different preparations.[3r] This cluster **2** can be envisaged as a capped three-shell 145-atom palladium core of pseudo-icosahedral I_h symmetry. Its metal core consists of a central Pd atom surrounded by an icosahedron of 12 Pd atoms (shell 1), that in turn are encapsulated by a ν_2 icosahedron of 42 Pd atoms (shell 2) (where ν_2 denotes $2 + 1 = 3$ equally spaced atoms on each of the 30 edges), that in turn are encapsulated by a rhombicosidodecahedron, a semi-regular Archimedean polyhedron, of 60 equiv Pd atoms (shell 3). Thirty additional Pd atoms cap the 30 quasi-square polygons of the third-shell polyhedron with a triethylphosphine ligand attached to each capping Pd atom. It is currently presumed that 60 COs (crystal-disordered) edge-bridge the 30 capping Pd atoms with one-half of the square basal Pd atoms (in accordance with a solid-state IR carbonyl spectrum). The pseudo-I_h Pd_{145} core has also been described by Alvarez[5] in terms of only radially equivalent vertex atoms as a Pd-centered five-shell system with the following successive polyhedral-nesting sequence: $Pd@Pd_{12}$(icosahedron)@Pd_{30}(icosidodecahedron)@Pd_{12}(icosahedron)@Pd_{60}(rhombicosidodecahedron)@Pd_{30}(capping icosidodecahedron). The diameter of the entire Pd_{145} core between two centrosymmetrically opposite capping Pd atoms is 1.65 nm; the diameter of the spheroidal-shaped geometry of the centered three-shell Pd_{115} kernel (i.e., without the 30 capping Pd atoms) is ca. 1.25 nm. Two other intriguing byproducts, $Au_2Pd_{41}(CO)_{27}(PEt_3)_{15}$[6] and $Au_2Pd_{21}(CO)_{20}(PEt_3)_{10}$,[7] were then isolated[3r] in moderate yields and crystallographically analyzed. More recently, a structure-to-synthesis approach resulted in the Au-centered hexacapped-cuboctahedral (ν_2 octahedral) Au_2Pd_{21} cluster[7] (with four exopolyhedral Pd atoms) being isolated in sufficient yields (60−70%) that permitted $^{31}P\{^1H\}$ NMR and electrochemical characterization.

After many attempts to increase the microscopic yields of the Pd_{145} cluster (**2**), a synthetic breakthrough was ultimately achieved by use of $Pd_{10}(CO)_{12}(PEt_3)_6$ in the absence of $Au(PPh_3)Cl$; the indicated yields, although still low (<10%), are somewhat larger with no byproduct Au−Pd contamination.[8] Magnetic circular dichroism measurements (4−30 K) of a powder sample definitely indicate **2** to be diamagnetic.[8]

Extensive efforts without prior success have been made to prepare other *multi-shell homopalladium* CO/PR_3-ligated clusters. Because PR_3 ligands with bulky R substituents are generally found to give rise to clusters with smaller Pd_n core-geometries, attempts primarily have involved reactions of palladium precursors with small-sized PEt_3,[3a,b,f,h−l,n,o,q] PMe_3,[3 g,p] and PMe_2Ph[3i] ligands.

"Full" *n*-shell sequences involving normal vertex-(edge-shared) shell-growth with the total number of atoms in a complete n^{th} shell being $(10n^2 + 2)$ are responsible for proposed

(1) For reviews, see: (a) Femoni, C.; Iapalucci, M. C.; Kaswalder, F.; Longoni, G.; Zacchini, S. *Coord. Chem. Rev.* **2006**, *250*, 1580. (b) Belyakova, O. A.; Slovokhotov, Yu. L. *Russ. Chem. Bull.* (Engl. Transl.) **2003**, *52*, 2299. (c) Collini, D.; Femoni, C.; Iapalucci, M. C.; Longoni, G.; Zanello, P. In *Perspectives in Organometallic Chemistry*; Screttas, C. G., Steele, B. R., Eds.; Special Publication No. 287, Royal Society of Chemistry: London, 2003; p 183. (d) Stromnova, T. A.; Moiseev, I. I. *Usp. Khim.* **1998**, *67*, 542. [*Russ. Chem. Rev.* (Engl. Transl.) **1998**, *67*, 485]. (e) Longoni, G.; Iapalucci, M. C. In *Clusters and Colloids: From Theory to Applications*; Schmid, G., Ed.; VCH Publ. Inc.: New York, 1994; pp 91−177. (f) Ceriotti, A.; Pergola, R. D.; Garlaschelli, L. In *Physics and Chemistry of Metal Cluster Compounds*; de Jongh, L. J., Ed.; Kluwer Academic Publ.: The Netherlands, 1994; Chapter 2, pp 41−106. (g) Burrows, A. D.; Mingos, D. M. P. *Transition Met. Chem.* **1993**, *18*, 129. (h) King, R. B. *Gazz. Chim. Ital.* **1992**, *122*, 383. (i) Eremenko, N. K.; Gubin, S. P. *Pure Appl. Chem.* **1990**, *62*, 1179. (j) Kharas, K. C. C.; Dahl, L. F. *Adv. Chem. Phys.* **1988**, *70*(Part 2), 1. (k) Eremenko, N. K.; Mednikov, E. G.; Kurasov, S. S. *Usp. Khim.* **1985**, *54*, 671. [*Russ. Chem. Rev.* (Engl. Transl.) **1985**, *54*, 394].

(2) (a) A comprehensive review was recently presented by Murahashi and Kurosawa[2b] on organopalladium complexes containing Pd-Pd bonding. (b) Murahashi, T.; Kurosawa, H. *Coord. Chem. Rev.* **2002**, *231*, 207.

(3) (a) Mednikov, E. G.; Eremenko, N. K.; Mikhailov, V. A.; Gubin, S. P.; Slovokhotov, Yu. L.; Struchkov, Yu. T. *J. Chem. Soc. Chem. Commun.* **1981**, 989. (b) Mednikov, E. G.; Eremenko, N. K.; Slovokhotov, Yu. L.; Struchkov, Yu. T.; Gubin, S. P. *J. Organometal. Chem.* **1983**, *258*, 247. (c) Mingos, D. M. P.; Hill, C. M. *Croat. Chem. Acta* **1995**, *68*, 745. (d) Mednikov, E. G.; Struchkov, Yu. T.; Slovokhotov, Yu. L. *J. Organometal. Chem.* **1998**, *566*, 15. (e) Kawano, M.; Bacon, J. W.; Campana, C. F.; Winger, B. E.; Dudeck, J. D.; Sirchio, S. A.; Scruggs, S. L.; Geiser, U.; Dahl, L. F. *Inorg. Chem.* **2001**, *40*, 2554. (f) Mednikov, E. G.; Slovokhotov, Yu. L.; Struchkov, Yu. T. *Metalloorgan. Khim.* **1991**, *4*, 123. [*Organomet. Chem. in the USSR* (Engl. Transl.) **1991**, *4*, 65]. (g) Tran, N. T.; Kawano, M.; Dahl, L. F. *J. Chem. Soc., Dalton Trans.* **2001**, 2731. (h) Mednikov, E. G.; Eremenko, N. K.; Slovokhotov, Yu. L.; Struchkov, Yu. T. *J. Organometal. Chem.* **1986**, *301*, C35. (i) Mednikov, E. G.; Wittayakun, J.; Dahl, L. F. *J. Cluster Sci.* **2005**, *16*, 429. (j) Mednikov, E. G.; Eremenko, N. K.; Slovokhotov, Yu. L.; Struchkov, Yu. T. *Zhurnal Vsesoyuzn. Khim. Obschestva im. D.I. Mendeleeva* (*Rus. J. Mendeleev's Chem. Soc.*) **1987**, *32*, 101. (k) Mednikov, E. G.; Ivanov, S. A.; Dahl, L. F. *Angew. Chem., Int. Ed.* **2003**, *42*, 323. (l) Mednikov, E. G.; Kanteeva, N. I. *Izv. Acad. Nauk. Ser. Khim.* **1995**, 167. [*Russ. Chem. Bull.* (Engl. Transl.) **1995**, *44*, 163]. (m) Mednikov, E. G.; Dahl, L. F., manuscript in preparation. (n) Mednikov, E. G.; Eremenko, N. K.; Slovokhotov, Yu. L.; Struchkov, Yu. T. *J. Chem. Soc. Chem. Commun.* **1987**, 218. (o) Mednikov, E. G.; Ivanov, S. A.; Slovokhotova, I. V.; Dahl, L. F. *Angew. Chem., Int. Ed.* **2005**, *44*, 6848. (p) Tran, N. T.; Kawano, M.; Powell, D. R.; Dahl, L. F. *J. Am. Chem. Soc.* **1998**, *120*, 10986. (q) Tran, N. T.; Dahl, L. F. *Angew. Chem., Int. Ed.* **2003**, *42*, 3533. (r) Tran, N. T.; Powell, D. R.; Dahl, L. F. *Angew. Chem., Int. Ed.* **2000**, *39*, 4121.

(4) Mednikov, E. G.; Ivanov, S. A.; Wittayakun, J.; Dahl, L. F. *J. Chem. Soc., Dalton Trans.* **2003**, 1686.

(5) Alvarez, S. *Dalton Trans.* **2005**, 2209, and references therein.

(6) Tran, N. T.; Powell, D. R.; Dahl, L. F. *J. Chem. Soc., Dalton Trans.* **2004**, 217.

(7) Tran, N. T.; Powell, D. R.; Dahl, L. F. *J. Chem. Soc., Dalton Trans.* **2004**, 209.

(8) Tran, N. T.; Dahl, L. F., unpublished results.

formulations of several noncrystalline giant full-shell palladium and platinum clusters stabilized by N/O-ligation: namely, five-shell Pd_{561} species independently by Moiseev and co-workers[9] and by Schmid,[10a−d] seven-/eight-shell Pd_{1451}/Pd_{2057} species by Schmid,[10e] and four-shell Pt_{309} species by Schmid.[10f] These giant-sized clusters, of which none has been isolated in single-crystal form, have been characterized by indirect methods including TEM, SAXS, EXAFS, ED, HREM, and elemental analysis. All contain anionic ligands at their surfaces, thereby suggesting that the metal surface layer may be partially oxidized. Moiseev, Vargaftik, and co-workers[11] have shown that the Pd_{561} clusters perform under mild conditions as catalysts in oxidation, redox disproportionation, and chain termination reactions. Catalytic properties of a number of other new Pd-containing nanoparticles have been reported,[12−14] and in particular one obtained from the molecular cluster precursor, $Pd_8(CO)_8(PMe_3)_7$.[15]

Herein we report the synthesis, isolation, and complete structural determination of the Pt-centered four-shell 165-atom Pd−Pt cluster, $(\mu_{12}\text{-Pt})Pd_{164-x}Pt_x(CO)_{72}(PPh_3)_{20}$, ($x \approx 7$), **1**. The approximate composition of its Pd−Pt core as a centered Pt atom with small random substitutions ($x \approx 7$) of Pd with Pt atoms in the inner three shells was established from estimated crystallographic Pt_xPd_{1-x} occupancies based upon least-squares refinement of the X-ray data. The total crystallographically estimated contribution of 8 ± 3 for the Pt atoms is consistent with that found from an X-ray Pt/Pd microanalysis (WDS spectrometer). SQUID magnetometry measurements of a single-crystal sample clearly established its diamagnetic behavior over 10−300 K. This unique example of a crystallographically proven four-shell metal-cluster structure of pseudo-icosahedral I_h symmetry and its detailed comparison with the structure of the Pd_{145} cluster (**2**) have produced a number of stereochemical surprises as well as provided considerable insight concerning our *bottom-up* synthetic approach in the formation and stabilization of truly monodispersed CO/PR_3-ligated homopalladium/hetero-palladium nanoparticles.

The closely similar interior 55-atom geometries of the composite central atom, shell 1 (12 atoms), and shell 2 (42 atoms) in **1** and **2** represent the first crystallographic examples of the well-known centered two-shell icosahedral Mackay hard-sphere model.[16] Also of interest is that the third-shell semi-regular pseudo-I_h polyhedron, rhombicosidodecahedron[5,17] (*vide infra*), possessed by the 60 equiv metal atoms in both **1** and **2**, is an otherwise crystallographically unknown stereoisomer of the semi-regular 60-atom vertex-truncated icosahedral polyhedron (with 12 pentagonal, 20 hexagonal faces)[5,17] observed for the universally familiar C_{60} buckminsterfullerene (buckyball).[18]

These nanosized clusters also have direct geometrical relevance with larger noncrystalline naked/ligated Pd/Pt nanoparticles and consequently should particularly attract interest among scientists in nanoscience and nanotechnology.

Results and Discussion

Four-Shell Metal-Core Anatomy of 1 and Geometrical Relationship with 2. (a) General Comments. The metal core consists of a central Pt atom surrounded by four concentric shells containing 12 atoms (shell 1), 42 atoms (shell 2), 60 atoms (shell 3), and 50 atoms (shell 4). Figure 1 displays side and top views of the 165 Pd−Pt core of **1**, and Figure 2 gives a detailed description of its "full" platinum-centered four-shell anatomy under pseudo-I_h icosahedral symmetry. Table 1 presents the means and ranges of individual distances for the 13 different types of metal−metal bonding connectivities (i.e., all atoms in shells 1−3 are designated as Pd) in **1** under I_h symmetry that are based upon the atom-labeling metal-core growth pattern given in Figure 3 along one of the four crystallographic or six pseudo threefold axes. For comparison, the corresponding means and ranges of analogous types of metal−metal distances are also given for the geometrically related **2** (i.e., M(A) denotes the centered Pt in **1** and Pd in **2**). This table reveals that the dispersion of individual metal−metal bonding separations for each of the means is unusually small. It also shows that the corresponding averages (means) for the 11 different types of metal−metal distances (i.e., 1 M(A)−Pd; 10 Pd−Pd) between **1** and **2** encompassing their equivalent shells 1, 2, and 3 agree within 0.03 Å except for the two types of Pd(E)−Pd(E) connectivities within shell 3; their highly significant differences in connectivity means are discussed later (*vide infra*).

(b) Structural Features of Shells 1 and 2: Analogy with 55-Atom Centered Two-Shell Mackay Icosahedral Model and Resulting Implications. The first two shells in **1** geometrically parallel those found in **2**. Shell 1 (Figure 2a) consists of a 12-atom ν_1 icosahedron that surrounds the central atom (where ν_n denotes $(n + 1)$ equally spaced atoms along each

(9) (a) Vargaftik, M. N.; Zagorodnikov, V. P.; Stolyarov, I. P.; Moiseev, I. I.; Likholobov, V. A.; Kochubey, D. I.; Chuvilin, A. L.; Zaikovsky, V. I.; Zamaraev, K. I.; Timofeeva, G. I. *J. Chem. Soc., Chem. Commun*. **1985**, 937. (b) Vargaftik, M. N.; Kozitsyna, N. Yu.; Cherkashina, N. V.; Rudy, R. I.; Kochubey, D. I.; Moiseev I. I. In *Metal Clusters in Chemistry*; Braunstein, P., Oro, L. A., Raithby, P. R., Eds.; Wiley-VCH: New York, 1999; Vol. 3, p 1364, and references therein.

(10) (a) Schmid, G. *Polyhedron* **1988**, *7*, 2321. (b) Schmid, G. *Chem. Rev*. **1992**, *92*, 1709, and references therein. (c) Schmid, G. In *Physics and Chemistry of Metal Cluster Compounds*; de Jongh, L. J., Ed.; Kluwer Academic Publ.: The Netherlands, 1994; Chapter 3, pp 107−134. (d) Schmid, G. In *Clusters and Colloids: From Theory to Applications*; Schmid, G., Ed.; VCH Publ. Inc.: New York, 1994; pp 178−211. (e) Schmid, G.; Harms, M.; Malm, J.-O.; Bovin, J.-O.; van Ruitenbeck, J.; Zandbergen, H. W.; Fu, W. T. *J. Am. Chem. Soc*. **1993**, *115*, 2046. (f) Schmid, G.; Morun, B.; Malm, J.-O. *Angew. Chem., Int. Ed. Engl*. **1989**, *28*, 778.

(11) (a) Kovtun, G.; Kameneva, T.; Hladyi, S.; Starchevsky, M.; Pazdersky, Yu.; Stolarov, I.; Vargaftik, M.; Moiseev, I. *Adv. Synth. Catal*. **2002**, *344*, 957. (b) Starchevsky, M. K.; Hladiy, S. L.; Pazdersky, Yu. A.; Vargaftik, M. N.; Moiseev, I. I. *J. Mol. Catal. A* **1999**, *146*, 229. (c) Moiseev, I. I.; Stromnova, T. A.; Vargaftik, M. N.; Orlova, S. T.; Chernysheva, T. V.; Stolarov, I. P. *Catal. Today* **1999**, *51*, 595. (d) Moiseev, I. I.; Vargaftik, M. N. In *Catalysis by Di- and Polynuclear Metal Cluster Complexes*; Adams, R. D.; Cotton, F. A.; Eds. Wiley-VCH: New York, 1998; Chapter 12, p 395. (e) Vargaftik, M. N.; Zagorodnikov, V. P.; Stolarov, I. P.; Moiseev, I. I.; Kochubey, D. I.; Likholobov, V. A.; Chuvilin, A. L.; Zamaraev, K. I. *J. Mol. Catal*. **1989**, *53*, 315. (f) Moiseev, I. I.; Vargaftik, M. N. *New J. Chem*. **1998**, *22*, 1217.

(12) An excellent review by Astruc et al.[13] presents recent developments in the use of metal nanoparticles (NPs) as recyclable catalysts in organic syntheses including hydrogenation and C−C coupling reactions. This review includes the elegant studies by the Toshima group[14] who used poly(*N*-vynil;-2-pyrrolidone) (PVP) to stabilize bimetallic Au−Pd clusters with Au(core)/Pd(shell) structures that enhanced the catalytic properties of Pd NPs relative to those of PVP-stabilized homopalladium NPs.

(13) Astruc, D.; Lu, F.; Aranzaes, J. R. *Angew. Chem., Int. Ed*. **2005**, *44*, 7852.

(14) (a) Shiraishi, Y.; Ikenaga, D.; Toshima, N. *Aust. J. Chem*. **2003**, *56*, 1025. (b) He, J.-H.; Ichinose, I.; Kunitake, T.; Nakao, A.; Shiraishi, Y.; Toshima, N. *J. Am. Chem. Soc*. **2003**, *125*, 11034. (c) Sablong, R.; Schlotterbeck, U.; Vogt, D.; Mecking, S. *Adv. Synth. Catal*. **2003**, *345*, 333.

(15) (a) A cluster-derived palladium nanoparticle catalyst on mesoporous silica, that was prepared from the molecular Pd_8 precursor, $Pd_8(CO)_8(PMe_3)_7$, was recently shown by Behrens and Spittel[15b] to be about six times more active as a hydrogenation catalysts than conventionally prepared catalysts for liquid-phase hydrogenation of alkenes. (b) Behrens, S.; Spittel, G. *Dalton Trans.* **2005**, 868.

(16) (a) Mackay, A. L. *Acta Crystallogr*. **1962**, *15*, 916. (b) Ino, S. *J. Phys. Soc. Jap*. **1966**, *21*, 346. (c) Farges, J.; de Feraudy, M. F.; Raoult, B.; Torchet, G. *Acta Crystallogr. Sect. A*. **1982**, *38*, 656. (d) Kuo, K. H. *Struct. Chem*. **2002**, *13*, 221.

(17) O'Keeffe, M.; Hyde, B. G. *Crystal Structures: Patterns and Symmetry*; Mineralogical Society of America: Washington, DC, 1996; Chapter 5.

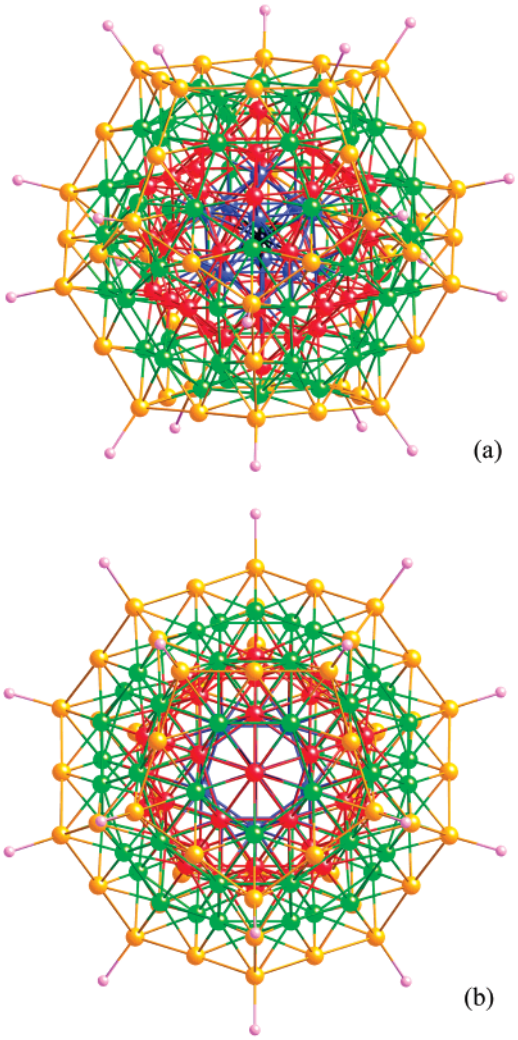

Figure 1. Side/top views of $(\mu_{12}\text{-Pt})Pd_{164-x}Pt_x(CO)_{72}P_{20}$ fragment in Pt-centered four-shell 165-atom Pd−Pt cluster, $(\mu_{12}\text{-Pt})Pd_{164-x}Pt_x(CO)_{72}(PPh_3)_{20}$ ($x \approx 7$), of pseudo icosahedral I_h ($2/m\bar{3}\bar{5}$) and cubic crystallographic T_h ($2/m\bar{3}$) site symmetry. (a) Side view showing four-shell geometry; (b) top view along one of six noncrystallographic $\bar{5}(S_{10})$ icosahedral axes passing through central (μ_{12}-Pt) atom, two centrosymmetrically opposite Pd(Pt) atoms in both shells 1 and 2, and midpoints of two centrosymmetrically opposite pairs of 12 pentagons within each shell 1, 2, 3, and 4.

edge). This centrosymmetrically centered icosahedron, which is one of the five Platonic solids (comprised of identical *regular* polygonal faces and *equivalent* vertices) has: (1) 6 5-fold axes through opposite pairs of 12 vertices; (2) 10 3-fold axes through midpoints of opposite pairs of 20 equiv triangular faces; and (3) 15 2-fold axes through midpoints of opposite pairs of 30 edges.

The second ν_2 icosahedral shell (Figure 2b) is composed of 42 atoms that can be formally derived by the addition of an atom to the midpoint of each of the 30 edges of the 12-atom ν_1 icosahedron. In the cluster growth process, the 42 atoms in shell 2 may be generated by the superposition of a six-atom ν_2 triangular face onto each ν_1 triangular face of the inner centered 13-atom icosahedron. The resulting composite 55-atom two-shell icosahedron has been previously designated as the well-known two-shell Mackay icosahedron,[16] which may be considered as 20 identical (slightly distorted) ν_2 tetrahedra that share a common vertex (i.e., the central atom) and are connected to one another through adjacent shared faces. Table 1 shows that the geometries of this Mackay icosahedron are virtually identical in **1** and **2**, which represent the only known crystallographic examples.[19] Noteworthy is that the formation of shells 1 and 2 conforms to the normal Mackay icosahedral vertex/(edge-shared) growth pattern involving an **abc**-atom sequence (*ccp* mode) along the 10 3-fold axes from the central atom to the corresponding 20 pairs of the parallel triangular ν_1 and ν_2 faces in shells 1 and 2, respectively.[20] The resulting total number of atoms in each "full" shell is $(10n^2 + 2)$.

(c) Structural Features of Semi-Regular Icosahedral 60-Atom Shell 3: Conformity to Anti-Mackay Third-Layer Icosahedral Atom-Arrangement and Stereochemical Relationship with Buckminsterfullerene (C_{60}). Mackay[16] proposed that the formation of the third shell of a normal icosahedral growth process required the arrangement of a 10-atom triangle (corresponding to a ν_3 equilateral triangle) above each ν_2 triangular face to give the 147-atom 3-shell icosahedron. However, shell 3 in both **1** and **2** instead involves the addition of only three atoms to the three equivalent internal sites of the 6-atom ν_2 triangular face of each of the 20 tetrahedra in the second shell to give a 60-atom polyhedron. Because shell 3 only has 60 atoms (instead of $10(3)^2 + 2 = 92$ atoms for the normal Mackay vertex-(edge-shared) shell growth), the three-shell part in both **1** and **2** possesses 115 atoms (instead of 147).

This alternative 115-atom three-shell core of **1** and **2** was actually postulated by Farges et al.[21] as a possible "full" shell structural model for charged noble-gas clusters formed in free-jet expansions into a vacuum, even though mass spectra of charged noble-gas clusters provide no subshell number evidence for an 115-atom cluster being particularly abundant because of special stability.[21,22] Farges et al.[21] recognized that this alternative third-shell coverage via face-capping of three atoms on each of the 20 ν_2 triangles in shell 2 gives rise to an ***abcb*** sequence (*hcp* mode). They designated this latter 115-atom three-shell cluster (without any capping atoms) as a *twin* arrangement to distinguish it from the 147-atom *regular* Mackay three-shell

(18) (a) Kroto, H. W.; Heath, J. R.; O'Brien, S. C.; Curl, R. F.; Smalley, R. E. *Nature* **1985**, *318*, 162. (b) Kräftschmer, W.; Lamb, L. D.; Fostiropoulos, K.; Huffman, D. R. *Nature* **1990**, *347*, 354. (c) Hou, J. G.; Zhao, A. D.; Huang, T.; Lu, S. In *Encyclopedia of Nanoscience and Nanotechnology*; Nalwa, H. S., Ed.; American Scientific Publishers: CA, 2004; Vol.1, pp 404−474.

(19) (a) Ab initio calculations[19b] of the total energies and relaxed geometries for "naked" gas-phase Pd_{55}, Ru_{55}, and Ag_{55} clusters showed an energy-difference preference for the Mackay 2-shell icosahedral geometry over the cuboctahedral (*fcc*) geometry. (b) Jenison, D. R.; Schultz, P. A.; Sears, M. P. *J. Chem. Phys.* **1997**, *106*, 1856.

(20) In contrast to a regular *ccp*/*hcp* metal arrangement where all metal−metal distances are equivalent, in a metal-centered icosahedral shell arrangement of I_h symmetry, the three tangential metal-metal edges in shell 1 are geometrically imposed to be ~5% larger than the three radial edges based upon angular strain considerations of the identically deformed 20 tetrahedra within an inner 13-atom centered icosahedral shell.[16a] This uniform contraction of the radial *vs* tangential edges is in complete agreement with the experimentally observed value of 5.3% (Table 1) for shell 1 in **1** {i.e., [(2.78 Å − 2.64 Å)/2.64 Å] × 100 = 5.3%}, as was also previously found in **2**. A similar 5.2% contraction is also observed for shell 2 in **1** {i.e., [(2.825 Å × 2) − (2.64 Å + 2.73 Å)/(2.64 Å + 2.73 Å)] × 100 = 5.2%}.

(21) (a) Farges, J.; de Feraudy, M. F.; Raoult, B.; Torchet, G. *J. Chem. Phys.* **1986**, *84*, 3491. (b) Farges, J.; de Feraudy, M. F.; Raoult, B.; Torchet, G. *Adv. Chem. Phys.* **1988**, *70*, 45.

(22) (a) Echt, O.; Sattler, K.; Recknagel, E. *Phys. Rev. Lett.* **1981**, *47*, 1121. (b) Harris, I. A.; Norman, K. A.; Mulkern, R. V.; Northby, J. A. *Chem. Phys. Lett.* **1986**, *130*, 316. (c) Northby, J. A. *J. Chem. Phys.* **1987**, *87*, 6166. (d) Lethbridge, P. G.; Stace, A. J. *J. Chem. Phys.* **1989**, *91*, 7687. (e) Lezius, M.; Scheier, P.; Stamatovic, A.; Mark, T. D. *J. Chem. Phys.* **1989**, *91*, 3240. (f) Kandler, O.; Leisner, T.; Echt, O.; Recknagel, E. *Z. Phys. D* **1988**, *10*, 295. (g) Miehle, W.; Kandler, O.; Leisner, T.; Echt, O. *J. Chem. Phys.* **1989**, *91*, 5940. (h) Echt, O.; Kandler, O.; Leisner, T.; Miehle, W.; Recknagel, E. *J. Chem. Soc. Faraday Trans.* **1990**, *86*, 2411.

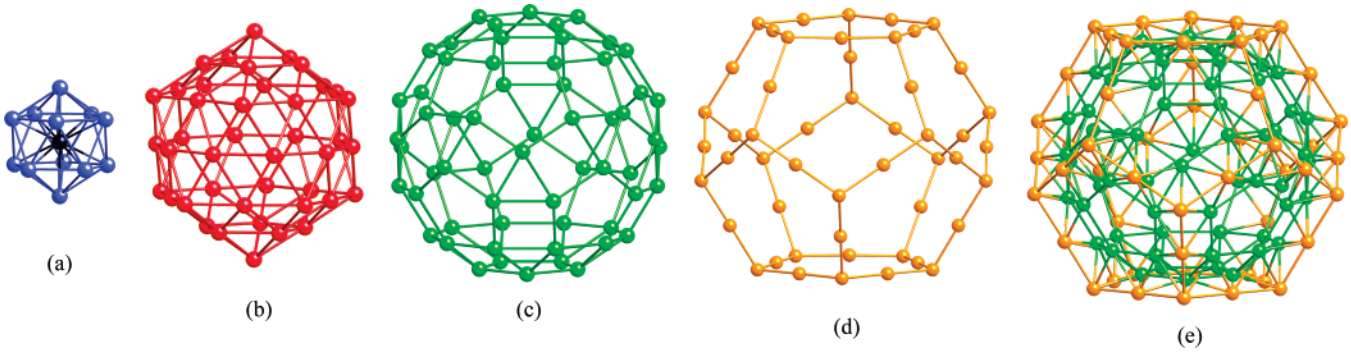

Figure 2. Four-shell anatomy of 165-atom Pt-centered Pt_xPd_{165-x} core ($x \approx 8$) in $(\mu_{12}\text{-Pt})Pd_{164-x}Pt_x(CO)_{72}(PPh_3)_{20}$ ($x \approx 7$), **1**. (a) shell 1 with central (μ_{12}-Pt) atom encapsulated by 12-atom Pt_xPd_{12-x} cage ($x \approx 1.2$); (b) shell 2 with 42-atom ν_2 icosahedral Pt_xPd_{42-x} cage ($x \approx 3.5$); (c) shell 3 with 60-atom semi-regular icosahedral Pt_xPd_{60-x} cage ($x \approx 2.2$), geometrically denoted as rhombicosidodecahedron (3.4.5.4); (d) shell 4 with 50-atom ν_2 pentagonal dodecahedral Pd_{50} cage; 20 PPh_3 ligands attached to 20 triangular-capping Pd vertices provide steric shielding of the metal core; (e) shell 3 encapsulated by shell 4, which has a geometrically "open" 50-atom dimple-ball metal surface that allows unprecedented cluster stabilization by *intershell* coordination of its 72 bridging CO ligands to both the second/third and third/fourth metal shells (Figure 4).

Table 1. Means/Ranges for Metal−Metal and Metal−Phosphorus Connectivities under Pseudo-I_h Icosahedral Symmetry in $(\mu_{12}\text{-Pt})Pd_{164-x}Pt_x(CO)_{72}(PPh_3)_{20}$, $x \approx 7(1)$ versus Corresponding Means/Ranges (in Brackets) in Geometrically Related $Pd_{145}(CO)_x(PEt_3)_{30}$, $x \approx 60(2)$[a]

connectivity[b,f]	N[c]	mean [Å][d]	range [Å][d]
M(A)−Pd(B)	12	2.64 {2.63}	2.642(3) {2.629(3)−2.633(3)}
Pd(B)−Pd(B)	30	2.78 {2.77}	2.763(4)−2.781(4) {2.757(4)−2.778(5)}
Pd(B)−Pd(C)	12	2.73 {2.74}	2.732(5) {2.734(4)−2.737(4)}
Pd(B)−Pd(D)	60	2.73 {2.70}	2.725(3−2.733(3) {2.696(4)−2.709(4)}
Pd(C)−Pd(D)	60	2.825 {2.82}	2.816(5)−2.832(5) {2.811(6)−2.836(6)}
Pd(D)−Pd(D)	60	2.84 {2.82}	2.839(5)−2.844(5) {2.810(5)−2.825(6)}
Pd(C)−Pd(E)	60	2.70 {2.73}	2.695(4)−2.709(6) {2.714(7)−2.749(7)}
Pd(D)−Pd(E)	120	2.77 {2.74}	2.765(4)−2.775(4) {2.724(6)−2.756(6)}
Pd(E)−Pd(E) (triangle/square shared edge)	60	2.99 {2.82}	2.987(5)−3.000(6) {2.795(8)−2.844(9)}
Pd(E)−Pd(E) (pentagonal/square shared edge)	60	3.02 {3.09}	3.013(6)−3.027(6) {3.070(8)−3.112(9)}
Pd(E)−Pd(F)	120	2.70 {2.84}	2.691(5)−2.714(4) {2.809(9)−2.874(9)}
Pd(E)−Pd(G)	60	2.76	2.758(5)−2.782(6)
Pd(F)−Pd(G)	60	3.085	3.065(5)−3.113(5)
Pd(G)−P[e]	20 {30}	2.29 {2.32}	2.290(12)−2.298(16) {2.181(13)−2.363(15)}

[a] All Atoms in Shells 1−3 in **1** Are Designated as Pd. Atom-labeling is given in Figure 3. [b] Central M(A) denotes Pt in **1** and Pd in **2**. [c] *N* denotes the number of symmetry-equivalent connectivities under I_h symmetry. [d] Means/ranges in brackets designate crystallographic values found for crystal A in **2**.[e] 20 PPh_3 ligands in **1** are attached to 20 triangular-capped Pd(G) vertices in shell 4, whereas in **2** these 20 Pd(G) atoms are absent and 30 PEt_3 ligands are attached to 30 square-capped Pd(F) atoms. [f] Labeled distances under assumed I_h symmetry correspond to the following crystallographic independent distances in **1**: M(A)−Pd(B): Pt(0)−Pd(1); Pd(B)−Pd(B): Pd(1)−Pd(1); Pd(B)−Pd(C): Pd(1)−Pd(3); Pd(B)−Pd(D): Pd(1)−Pd(2), Pd(1)−Pd(4); Pd(C)−Pd(D): Pd(2)−Pd(3), Pd(3)−Pd(4); Pd(D)−Pd(D): Pd(2)−Pd(4), Pd(4)−Pd(4); Pd(C)−Pd(E): Pd(3)−Pd(5), Pd(3)−Pd(6), Pd(3)−Pd(7); Pd(D)−Pd(E): Pd(2)−Pd(7), Pd(4)−Pd(5), Pd(4)−Pd(6), Pd(4)−Pd(7); Pd(E)−Pd(E) (t/s): Pd(5)−Pd(5), Pd(6)−Pd(7), Pd(7)−Pd(7); Pd(E)−Pd(E) (p/s): Pd(5)−Pd(6), Pd(5)−Pd(7), Pd(7)−Pd(7); Pd(E)−Pd(F): Pd(5)−Pd(8), Pd(6)−Pd(8), Pd(7)−Pd(8), Pd(7)−Pd(9); Pd(E)−Pd(G): Pd(5)−Pd(10), Pd(6)−Pd(11), Pd(7)−Pd(11); Pd(F)−Pd(G): Pd(8)−Pd(10), Pd(8)−Pd(11), Pd(9)−Pd(11); Pd(G)−P: Pd(10)−P(1), Pd(11)−P(2).

arrangement. This latter *regular* atom-site arrangement for shell 3 has also been denoted as edge-capping/vertex (ECV3)[22b,c] or the *Mackay* overlayer,[23] whereas the *twin* arrangement for shell 3 has been denoted as face-capping/vertex (FCV3)[22b,c,24] or the *anti-Mackay* layer.[23]

The third shell of **1** (Figure 2c), in contrast to that of **2** (*vide infra*), experimentally conforms to a semiregular (Archimedean) polyhedron[5,17] that contains 60 *equivalent vertices* and three *regular polygons with all sides having the same length*. The polygons consist of 12 pentagonal, 20 triangular, and 30 square faces with each side of the 12 pentagons and 20 triangles being edge-bridged to one of the 30 squares; the resulting 120 edges of the rhombicosidodecahedron thereby possess 60 pentagon/square and 60 triangle/square edges. This 60-atom polyhedron is mathematically named rhombicosidodecahedron (3.4.5.4), where the numbers (*N*) in parentheses denote the Schläfli symbol, which represents in cyclic order the polygons (*N*-gons) joined at each equivalent vertex.[17]

The most important stereochemical consequence of this third-shell M_{60} arrangement (over the two-shell regular M_{55} icosahedral metal core) is that it is not feasible without significant *elongation* of at least one-half of its M−M connectivities up to 3.0 Å. In fact, in **1**, all 120 tangential M−M edge-connectivities (means: 2.99, 3.02 Å) lie in the weakly bonding but yet amazingly narrow range of 2.987(5)−3.027(6) Å (Table 1), thereby closely conforming geometrically to an *ideal* Archimedean rhombicosidodecahedral polyhedron M_{60} with *regular* triangular, square, and pentagonal *N*-gons [3.4.5.4] about each of the 60 equiv vertices. On the other hand, in **2**, only one-half of the 120 surface edge connectivities, namely, the 60 common pentagon/square edges, are similarly elongated (mean, 3.09 Å; range, 3.070(8)−3.112(9) Å), whereas the other 60 common triangle/square edges have considerably smaller lengths (mean, 2.82 Å; range 2.795(8)−2.844(9) Å). These two distinctly

(23) (a) Wales, D. J.; Munro, L. J.; Doye, J. P. K. *J. Chem. Soc. Dalton Trans.* **1996**, 611. (b) Wales, D. J.; Doye, J. P. K. *J. Phys. Chem. A* **1997**, *101*, 5111. (c) Doye, J. P. K.; Wales, D. J. *J. Chem. Soc. Faraday Trans.* **1997**, *93*, 4233, and references therein.

(24) The complete third shell was considered as a 72-atom (instead of the 60-atom) polyhedron (of I_h symmetry) consisting of the 60 face-capping vertices at stacking-fault locations (i.e., the rhombicosidodecahedron) and 12 additional pentagonal-capped vertices.[22b,c]

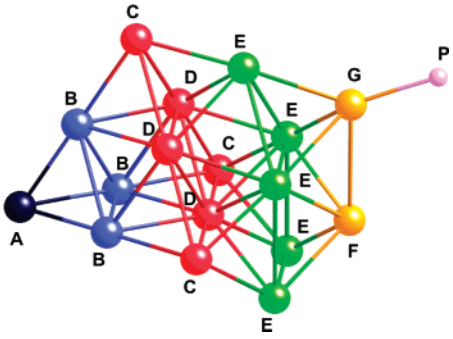

Figure 3. Shell-by-shell metal-core growth pattern (with designated atom-labeling in connection with Table 1) depicted along one of 10 threefold axes of pseudo-I_h icosahedral symmetry in the M(A)-centered four-shell 165-atom Pt−Pd core in **1** (with M(A) = Pt and with all atoms in shells 1, 2, 3 designated as Pd) and in the M(A)-centered capped three-shell 145-atom Pd core in **2** (with M(A) = Pd). In **1** the 20 triangular-capped Pd(G) atoms in ν_2 pentagonal dodecahedral shell 4 are coordinated to PPh_3 ligands, whereas in **2** these 20 Pd(G) atoms are absent and 30 PEt_3 ligands are instead coordinated to the 30 square-capped Pd(F) atoms. In this figure, the 3-fold axis passes through the central M(A) atom, the midpoint of the Pd(B) triangle in shell 1, the midpoint of the inner Pd(D) triangle in shell 2, the midpoint of the Pd(E) triangle in shell 3, the triangle-capping Pd(G) atom in shell 4, and its attached P(G) atom in **1** (i.e., these latter Pd(G) and P(G) atoms are absent in **2**). A horizontally oriented 2-fold axis in this figure passes through the central M(A) atom, the midpoint of two edge-connected Pd(B) atoms in shell 1, one Pd(D) atom in shell 2, the midpoint of the Pd(E) quasi-square polygon in shell 3, the square-capping Pd(F)atom in shell 4, and its attached P(F) atom in **2** (absent in **1**).

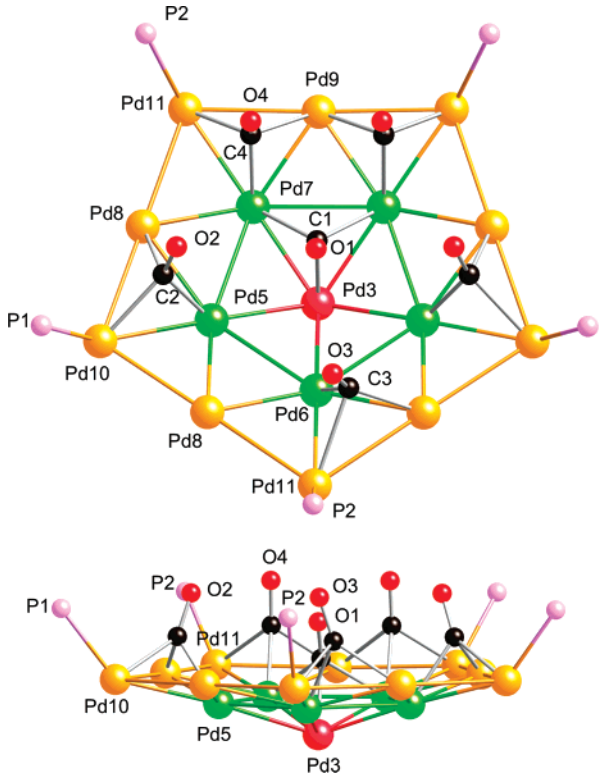

Figure 4. Top/side views showing distribution of 72 bridging carbonyl ligands in **1** as six *intershell* bridging COs within one of the 12 symmetry-equivalent pentagons of the ν_2 pentagonal dodecahedral Pd_{50} polyhedron of shell 4. Atom-labeling corresponds to the crystallographic independent unit—namely, 1 central Pt, 11 Pd, 2 P atoms, and 4 COs. Because each of the two (body centered)-related clusters (**1**) in the cubic unit cell has T_h ($2/m\bar{3}$) site symmetry, the independent part is composed of one-half pentagon that has a mirror plane passing through Pd(9), Pd(11) and its attached P(2) of shell 4, Pd(6) of shell 3, and Pd(3) of shell 2. The central C(1)O(1) ligand lying on the mirror plane links shells 2 and 3, whereas each of the outer five CO ligands (three independent) links shells 3 and 4; only one orientation of the crystal-disordered C(3)O(3) ligand is shown. Under I_h symmetry, Pd(3) is designated as a vertex Pd(C) atom, Pd(5), Pd(6), Pd(7) are denoted as Pd(E) atoms, Pd(8), Pd(9) as Pd(F) atoms, and Pd(10), Pd(11) as Pd(G) atoms.

dissimilar types of M−M connectivities (that differ by a mean value of 0.27 Å) result in the conversion of *regular* square polygons into rectangular ones, thereby resulting in the distortion of the Pd_{60} polyhedron from being an Archimedean rhombicosidodecahedron (by definition),[17,25] even though the localized icosahedral I_h symmetry of the third shell is maintained (i.e., under I_h symmetry each rectangular face still possesses a perpendicular 2-fold axis passing through its midpoint). The observed difference is readily attributed to the equalizing effect of the outer shell 4 in **1** composed of 50 *virtually equal-distance interconnected* Pd atoms which cap *both the triangular and square* faces of shell 3 (*vide infra*) versus only 30 mutually *non-connected* square-capping Pd atoms in **2**. An intrinsic structural feature of shell 3 in both **1** and **2** is that the rhombicosidodecahedral pentagonal faces are "open" (i.e., the mean M−M edge-connectivities are 3.02 and 3.09 Å, respectively), making the pentagonal vertices of shell 2 accessible for intershell bridging ligation (*vide infra*).

Particularly noteworthy is that the third-shell rhombicosidodecahedral polyhedron of 60 atoms is a stereoisomer of the truncated icosahedral Buckminsterfullerene C_{60} molecule (buckyball),[18] another one of the five icosahedral Archimedean polyhedra possessing I_h symmetry.[17,25] This truncated icosahedral polyhedron with 60 equiv vertices and 12 pentagonal and 20 hexagonal faces may be formally derived by vertex-truncation of an icosahedron at one-third of each of its 30 edges, such that the 12 vertices are transformed into 12 regular pentagons and the 20 triangles are transformed into 20 regular hexagons.

(d) Structural Features of 50-Atom ν_2 Pentagonal Dodecahedral Shell 4 and Resulting Implications. The 50-atom shell 4 in **1** constitutes a ν_2 pentagonal dodecahedron, a regular Platonic solid containing 20 vertices (namely, the 20 Pd(G) atoms in Figure 3 that correspond to the crystallographically independent Pd(10), Pd(11) atoms in Figure 4) and 12 pentagonal faces (i.e., the "dual" of a ν_1 icosahedron involving an interchange of vertices and faces). The midpoints of the 30 pentagonal edges are additionally occupied by atoms (namely, the 30 Pd(F) atoms in Figure 3 that correspond to the independent Pd(8), Pd(9) atoms in Figure 4). The 20 vertex Pd(G) atoms cap all triangular faces of shell 3, whereas 30 Pd(F) midpoint-edge atoms cap its square faces. Although these 50 atoms are linked at distances (Pd(F)−Pd(G) mean, 3.085 Å) corresponding to weak bonding interactions (i.e., the Pd−Pd distance in ccp Pd metal is 2.75 Å),[26] the ν_2 pentagonal dodecahedron is amazingly regular. The Pd(F)−Pd(G) distances (Table 1) span a narrow range of 3.065(5)−3.113(5) Å, and the nonbonding vertex−vertex Pd(G)−Pd(G) separations are virtually equivalent (range, 6.14−6.17 Å). Furthermore, each ν_2 pentagon (Figure 4), defined by the 10 Pd(F), Pd(G) atoms under I_h symmetry, is essentially planar; the perpendicular deviations of the five vertex Pd(G) atoms (i.e., Pd(10), Pd(11))

(25) (a) Wenninger, M. J. The Thirteen Semiregular Convex Polyhedra and Their Duals. In *Dual Models*; Cambridge University Press: Cambridge, England, 1983; Chapter 2, pp 14−35. (b) Weisstein, E. W. Semiregular Polyhedron."In *MathWorld*; A Wolfram Web Resource. http://mathworld.wolfram-.com/SemiregularPolyhedron.html].
(26) Donohue, J. *The Structures of the Elements*; John Wiley & Sons: New York, 1974; p 216.

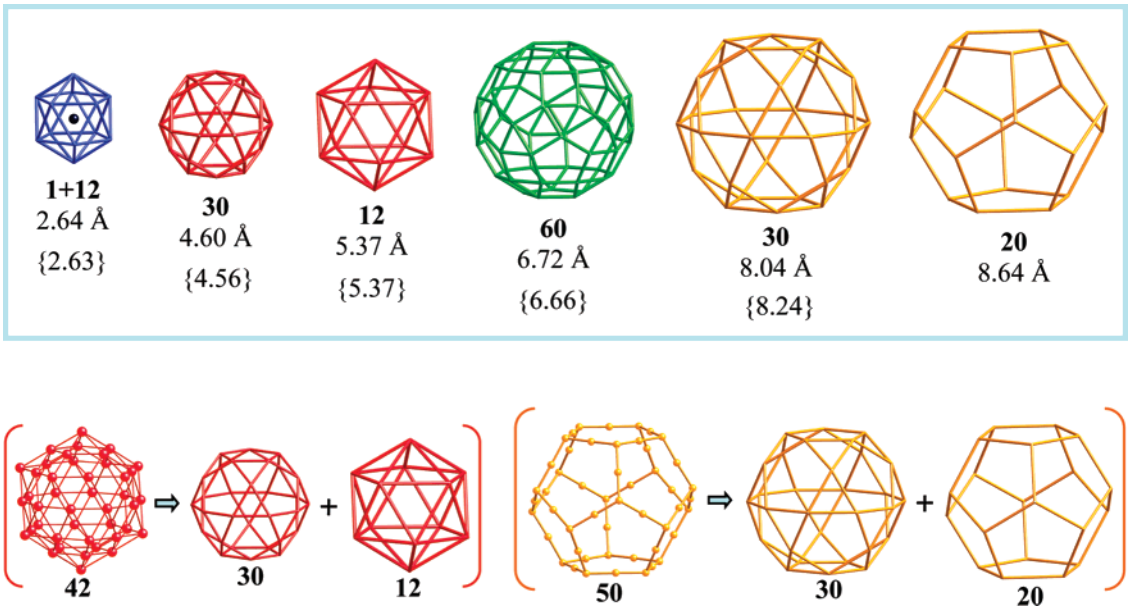

Figure 5. Complementary Pt-centered six-shell successive polyhedral description of (μ_{12}-Pt)M_{164} core-geometry of **1** having only equivalent *vertex atoms* under pseudo-icosahedral I_h symmetry: Pt@M_{12}(icosahedron)@M_{30}(icosidodecahedron)@M_{12}(icosahedron)@M_{60}(rhombicosidodecahedron)@M_{30}(icosidodecahedron)@M_{20}(pentagonal dodecahedron). Six successive concentric Platonic/Archimedean polyhedra encapsulate the central Pt atom. Radial shell distances between the central Pt atom and equivalent vertices are given below the number of atoms in each shell. Corresponding radial shell distances for **2** are given in brackets. An Archimedean M_{30} icosidodecahedron (3.5.3.5) is generated via midpoint truncation of either an icosahedron (3^5) or pentagonal dodecahedron (5^3); consequently, a ν_2 M_{42}(icosahedron) is transformed into M_{30}(icosidodecahedron) + M_{12}(icosahedron), and likewise a ν_2 M_{50}(pentagonal dodecahedron) is transformed into M_{30}(icosidodecahedron) + M_{20}(pentagonal dodecahedron).

from the 10-atom mean plane are only 0.003−0.01 Å, whereas those of the five edge-sided midpoint Pd(F) atoms (i.e., Pd(8), Pd(9)) are 0.01−0.06 Å larger.

Formation of the ν_2 pentagonal dodecahedron containing only 50 Pd atoms is a consequence of the additional 20 Pd atoms capping the 20 triangular faces (Figure 2c) of the rhombicosidodecahedral polyhedron (shell 3) that creates 20 triphenylphosphine-attached Pd vertices in shell 4 which are necessarily indirectly linked to one another via the 30 square-capped Pd atoms at the midpoints of the 30 pentagonal edges of shell 4. The resulting diameter of the entire spheroidal-shaped metal-core of **1** between two centrosymmetrically opposite vertices of the ν_2 pentagonal dodecahedron is 1.73 nm.

To our knowledge, the Pd_{50} architecture of shell 4 is the first example of a ν_2 pentagonal dodecahedron, whereas a few molecular ν_1 pentagonal dodecahedra are known or theoretically postulated. These include the remarkable, synthetic-challenging hydrocarbon, $C_{20}H_{20}$ (corresponding to a "Mount Everest" ascent), and its derivatives obtained by Paquette, et al.,[27] and recently Si_{20} cages (as one of two different fullerene-like Si_n polyhedra) in alkali metal silicon clathrates: Na_8Si_{46}[28a] (along with Si_{24} cages), and Na_xSi_{136}, ($x = 4-23$),[28a] $Rb_8Na_{16}Si_{136}$,[28b] and $Cs_8Na_{16}Si_{136}$[28b] (along with Si_{28} cages); corresponding pentagonal dodecahedral Ge_{20} cages are found in the structurally analogous germanium clathrates, $Rb_8Na_{16}Ge_{136}$,[28b] and $Cs_8Na_{16}Ge_{136}$.[28b] The synthesis and structural/bonding study of $[As@Ni_{12}@As_{20}]^{3-}$ ($[PBu_4]^+$salt),[29] in which an As_{20} pentagonal dodecahedron encapsulates the As-centered "dual" Ni_{12} icosahedron, triggered DFT calculations[30] of this cluster and its hypothetical Sb/Pd congener, $[Sb@Pd_{12}@Sb_{20}]^{3-}$ anion.[30b]

A Au_{20} pentagonal dodecahedron that encapsulates the Mn-centered "dual" Mn_{12} icosahedron in the hypothetical $[Mn_{13}@Au_{20}]^-$ anion has been reported[31] this year from DFT calculations; the postulated ultrahigh magnetic moment of this gold-coated cluster is predicted to be an order of magnitude higher than that of the "bare" $Mn_{13}-$ core *per se*.[31,32]

(e) Complementary Six-Shell Description of (μ_{12}-Pt)M_{164} Core in 1. An alternative description of nested (concentric) multi-shell ν_1 Platonic/Archimedean polyhedra with only symmetry-equivalent vertex atoms in clusters and in the solid state has recently been put forth by Alvarez[5] in a superb comprehensive, historically enriched review of polyhedra in (inorganic) chemistry. Alvarez[5] views the capped three-shell spheroidal-shaped Pd_{145} core of **2** as a concentric polyhedral composite of five shells with the following nesting sequence: Pd_{12}-icosahedron@Pd_{30}-icosidodecahedron@Pd_{12}-icosahedron@Pd_{60}-rhombicosidodecahedron@Pd_{30} (capping)-icosidodecahedron.

In a similar fashion (Figure 5), the 165-atom (μ_{12}-Pt)M_{164} core-geometry of **1** may likewise be generated by a six-shell polyhedral growth pattern of pseudo-I_h symmetry about the central Pt atom, such that each ν_1 polyhedron corresponds to a shell of only symmetry-equivalent vertex atoms at a certain radial distance from the Pt atom. The successive "matryoshka"-doll sequence of each polyhedron and its radial Pt−M shell distance are as follows: Pt@M_{12}-icosahedron [Pt−M(B), 2.64

(27) (a) Paquette, L. A.; Ternansky, R. J.; Balogh, D. W.; Kentgen, G. *J. Am. Chem. Soc*. **1983**, *105*, 5446. (b) Paquette, L. A.; Weber, J. C.; Kobayashi, T.; Miyahara, Y. *J. Am. Chem. Soc*. **1988**, *110*, 8591, and references therein.
(28) (a) Ramachandran, G. K.; Dong, G.; Diefenbacher, J.; Gryko, J.; Marzke, R. F.; Sankey, O. F.; McMillan, P. F. *J. Solid State Chem*. **1999**, *145*, 716. (b) Bobev, S.; Sevov, S. C. *J. Solid State Chem*. **2000**, *153*, 92.
(29) Moses, M. J.; Fettinger, J. C.; Eichhorn, B. W. *Science*, **2003**, *300*, 778.
(30) (a) Baruah, T.; Zope, R. R.; Richardson, S. L.; Pederson, M. R. *Phys. Rev. B* **2003**, *68*, 241404. (b) Zhao, J.; Xie, R.-H. *Chem. Phys. Lett*. **2004**, *396*, 161. (c) King, R. B.; Zhao, J. *Chem. Commun*. **2006**, 4204.
(31) Wang, J.; Bai, J.; Jellinek, J.; Zeng, X. C. *J. Am. Chem. Soc*. **2007**, *129*, 4110.
(32) (a) By use of Pt-mediated, coordination-driven self-assembly of predesigned directional-binding complementary subunits (viz., 30 ditropic with ∼180° edges) and 20 tritropic with ∼108° vertices), Stang and co-workers[32b,c] have successfully synthesized quantitatively two +60-charged metallocyclic caged structures consisting of conformationally rigid pentagonal dodecahedral polyhedra of nanosized dimensions (i.e., ∼0.5 and ∼0.8 nm in outer sizes). (b) Olenyuk, B.; Levin, M. D.; Whiteford, J. A.; Shield, J. E.; Stang, P. J. *J. Am. Chem. Soc*. **1999**, *121*, 10434. (c) Seidel, S. R.; Stang, P. J. *Acc. Chem. Res*. **2002**, *35*, 972.

Table 2. Equivalent Isotropic Atomic Displacement Means/Ranges for Independent Metal(Core) and P Atoms in Four-Shell (μ_{12}-Pt)$Pd_{164-x}Pt_xP_{20}$ Fragment of **1** versus Corresponding Means (in Brackets) for Independent Metal(Core) and P Atoms in Geometrically Related Capped Three-Shell $Pd_{145}P_{30}$ Fragment of **2**[a]

independent atoms[b]	mean (Å)	range(Å)
central M(A)		
M(A) = Pt in **1**, Pd in **2**	0.067 {0.063}	–
shell 1:		
12Pd(B): [12Pd(1)]	0.071	–
	{0.080}	{0.079−0.080}
shell 2:		
30Pd(D): [6Pd(2); 24Pd(4)]	0.086	0.084−0.086
	{0.106}	{0.101−0.107}
12Pd(C): [12Pd(3)]	0.094	–
	{0.121}	{0.120−0.121}
shell 3:		
60Pd(E): [24Pd(5); 12Pd(6); 24Pd(7)]	0,118	0,116−0,120
	{0.156}	{0.150−0.165}
shell 4 in **1** {capping in **2**}:		
30Pd(F): [24Pd(8); 6Pd(9)]	0.150	0.146−0.168
	{0.229}	{0.217−0.231}
20Pd(G): [8Pd(10); 12Pd(11)]	0.150	0.145−0.157
20P(G): [8P(1); 12P(2)] in **1**	0.171	0.133−0.196
30P(F) in **2**	{0.289}	{0.276−0.304}

[a] All Atoms in Shells 1−3 in **1** Are Designated as Pd. Values for both **1** and **2** were obtained from anisotropic least-squares refinement of CCD X-ray data (Mo Kα) collected at 100 K. In **1** the crystallographically independent unit consists of 12 metal and two phosphorus atoms under cubic $2/m\bar{3}$ (T_h) site symmetry with the central Pt located at the inversion center. These independent atoms are classified under pseudo-I_h symmetry. In **2** the crystallographically independent unit consists of 25 Pd atoms and 5 P atoms under $\bar{3}$ (S_6) site symmetry with the central Pd atom located at the inversion center; under pseudo-I_h symmetry **2** is comprised of the central Pd(A) atom, two independent Pd(B) atoms in shell 1, two independent Pd(C) atoms and five independent Pd(D) atoms in shell 2, 10 independent Pd(E) atoms in shell 3, and five independent Pd(F) capping atoms and five independent attached P(F) atoms. [b] Atom-labeling is given in Figure 3 under pseudo-I_h symmetry.

Å] @M_{30}-icosidodecahedron [Pt−M(D), 4.60 Å] @M_{12}-icosahedron [Pt−M(C), 5.37 Å] @M_{60}-rhombicosidodecahedron [Pt−M(E), 6.72 Å] @M_{30}-icosidodecahedron [Pt−M(F), 8.04 Å] @M_{20}-pentagonal dodecahedron [Pt−M(G), 8.64 Å]. A comparison between radial M(A)-M(vertex) distances of corresponding polyhedra in **1** and **2** is also presented in Figure 5. As expected, the corresponding radial values are in reasonably close agreement, especially those for the inner polyhedra.

(f) Comparative Analysis of Relative Equivalent Isotropic Atomic Displacement Values of the Multi-Shell Metal Core-Phosphorus Fragments in the Cubic Crystal Structures of 1 and 2 and Resulting Implications. Equivalent isotropic atomic displacements of the independent atoms (from their equilibrium positions), obtained from anisotropic least-squares refinement of the independent central metal, 11 shell metal sites, and two P atoms in **1** under crystallographic $2/m\bar{3}$ (T_h) site symmetry are given in Table 2 along with those previously obtained[3r] for the independent 25 Pd and five P atoms in **2** under crystallographic $\bar{3}$ (S_6) site symmetry from the anisotropic refinement of the CCD X-ray data (Mo Kα) for crystal A, also collected at 100 K. These independent atoms in both **1** and **2** are classified under pseudo-I_h symmetry in accordance with the common atom-labeling given in Figure 3. Atomic coordinates, number of equivalent site positions, and crystallographic site symmetry for the central Pt atom, 11 independent metal shell atoms, two independent phosphorus atoms, four independent phenyl rings, and one independent solvated acetone molecule are presented in the Supporting Information (Table S1).

An examination of Table 2 reveals a parallel increase in both **1** and **2** of the equivalent isotropic atomic displacements from their equilibrium positions as a function of increased radial shell distance between the central metal atom and equivalent metal vertices (Figure 5). This trend coupled with the narrow ranges observed for each of the means in **1** and **2** are consistent with their spheroidal-like multi-shell geometries. Particularly noteworthy is that the corresponding relative means in shells 1−3 increase more rapidly with increased shell number in **2**, and that of 0.229 Å for the 30 capping Pd(F) atoms in **2** is considerably larger than those of 0.150 Å for both the 30 Pd(F) and 20 Pd(G) atoms in shell 4 of **1**. This trend together with the much larger relative mean of 0.289 Å for the 30 triethylphosphine P(F) atoms in **2** versus that of 0.171 Å for the 20 triphenylphosphine P(G) atoms in **1** may readily be ascribed to the much bulkier triphenylphosphine substituents and to the presence of solvated molecules in the crystal structure of **1**, that concomitantly greatly dampen the thermal motion of the Pd(G)-attached phosphorus P(G) atoms. The self-consistent results of this analysis of the atomic thermal parameters provide definite evidence that the multi-shell molecular structures of both **1** and **2** are presumed to oscillate about their equilibrium positions as relatively rigid compact spheres. This analysis is in accordance with the observed orientations of the anisotropic displacement ellipsoids of the crystallographically independent metal atoms being generally elongated along tangential shell directions relative to smaller radial displacements.

Distribution of Platinum Atoms in the $Pd_{165-x}Pt_x$ Core of 1 Based upon the Crystallographic Determination and X-Ray Pd/Pt Microanalyses of Single Crystals. A least-squares (Pt_xPd_{1-x})-occupancy site analysis of the X-ray diffraction data revealed the following site-disordered occupancies for the crystallographically independent atoms (namely, the central atom and those in shells 1−3): (1) the central atom was conclusively shown to be Pt in that the occupancy factor was $x = 1.00(3)$; (2) the icosahedral Pt_xPd_{12-x} cage in shell 1 was determined to consist of 1.2(3) Pt atoms and 10.8(3) Pd atoms on the basis of the occupancy $x/(1-x)$ factor of 0.10/0.90(2.0) found for the one independent site-disordered Pt(1)/Pd(1) position; (3) the 42-atom ν_2 icosahedral cage in shell 2, composed of the three independent Pt(2)/Pd(2), Pt(3)/Pd(3), and Pt(4)/Pd(4) site-disordered positions with occupancy factors of 0.06/0.94(2.5) (6 edge midpoints), 0.08/0.92(1.8) (12 vertices) and 0.09/0.91(1.4) (24 remaining edge midpoints), respectively, results in an estimated total Pt occupancy of 3.5(5) for all 42 positions; (4) analogously, for the 60-atom rhombicosidodecahedron in shell 3 the Pt/Pd site occupancy factor refinement for the three independent positions, Pt(5)/Pd(5) (24 vertices), Pt(6)/Pd(6) (12 vertices), and Pt(7)/Pd(7) (24 vertices) gave 0.04/0.96(1.5), 0.06/0.94(1.7), and 0.02/0.98(1.4), respectively; the resulting estimated total Pt occupancy in shell 3 is 2.2(6). Thus, the Pt compositional contribution from shell 1 to shell 3 progressively decreases from 10% (shell 1) to 8% (shell 2), and to 4% (shell 3), with the latter value being close to experimental uncertainty. The total number of estimated Pt atoms 8 ± 3, including the central Pt atom, is in fortuitous agreement with the atomic Pt/Pd ratio of 7.6(7)/157.4, found in an X-ray microanalysis performed on three crystals of **1** with a wavelength-

dispersive spectrometer (WDS), in which Pt and Pd metals were used as standards. A less accurate standardless X-ray microanalysis on scanning electron microscope with an energy-dispersive system (EDS) gave a Pt/Pd ratio in the range of (7.9−13.1)/(157.1−151.9), which, nevertheless, is still consistent with both the X-ray diffraction and WDS analysis.

It should be noted that our utilization of the site-occupancy (Pt_xPd_{1-x})-analysis for the independent atoms in shells 1−3 originated from results of the experimental Pt/Pd microanalysis; otherwise (in its absence), the presumed metal-core composition would have been given as (μ_{12}-Pt)Pd_{164}, especially in light of the fractional occupation of positions in the inner shells by Pt atoms being small (≤10%) and consequently on the borderline of significance. Also noteworthy is that (in general) a high correlation exists between the site occupancy factor *x* of an atom and its equivalent isotropic displacement parameter. Hence, the small compositional distribution of Pt metal atoms within shell 1 and especially within shells 2 and 3 should be considered as *idealized*. We also cannot completely rule out the presence of Pt atoms in shell 4, even though that contribution should be insignificant.

Stereochemistry of PPh_3/CO Ligation in 1. Refinement of the crystal structure of **1** revealed 20 PPh_3 ligands (two independent) attached to the 20 Pd(G) vertices of the ν_2 pentagonal dodecahedral together with 72 carbonyl ligands (four independent). Eight of the 20 PPh_3 ligands consist of equivalent Pd(10)-attached P(1) atoms (Table S1) with two centrosymmetrically related ones lying on each of the four body-diagonal crystallographic threefold cubic <111> axes that pass through the bonding Pd(10)−P(1) connectivities (labeled Pd(G)−P(G) in Figure 3). The three phenyl rings attached to each P(1) atom are thereby related by a threefold crystallographic axis and hence constitute one independent whole-weighted $C_6H_5(1)$ group (that was refined as a rigid body). The other 12 PPh_3 ligands consist of Pd(11)-attached P(2) atoms that possess mirror-plane site symmetry (Table S1). Hence, three independent P(2)-attached phenyl rings, $C_6H_5(2)$, $C_6H_5(3)$, $C_6H_5(4)$, are each disordered over two orientations by a mirror that passes through each of the 12 equiv Pd(11)−P(2) connectivities. (Each half-weighted phenyl ring was refined as a rigid group.)

Of major importance is that the exceedingly rare high cubic crystallographic site symmetry of $2/m\bar{3}$ (T_h) enabled the establishment of 72 bridging carbonyl ligands in **1** that were located as six bridging COs (four independent) within each of the 12 symmetry-equivalent pentagons of the ν_2 pentagonal dodecahedral Pd_{50} polyhedron of shell 4. Figure 4 displays both top/side views of one pentagon showing the distribution of carbonyl ligands with atom-labeling corresponding to the crystallographically independent atoms. The top view of this figure reveals that the pentagon has a mirror plane that passes through the vertex Pd(3) atom (red) of shell 2, the Pd(6) atom (green) of shell 3, and the Pd(9) and Pd(11) atoms (gold) of shell 4.

The most remarkable, geometrically unprecedented stereochemical feature of the carbonyls is that all of them are involved in *intershell* bonding. Figure 4 shows that C(1)O(1), lying on the mirror, links shells 2 and 3, and C(2)O(2), C(3)O(3), and C(4)O(4) connect shells 3 and 4. The binding of C(1)O(1) is of particular interest, because of its deep penetration in connecting shells 2 and 3; in fact, the vertex Pd(3) atom of shell 2 is located at 0.83 and 1.50 Å beneath the pentagons formed by the independent Pd(5), Pd(6), Pd(7) atoms in shell 3 and by the independent Pd(8), Pd(9), Pd(10), Pd(11) atoms in shell 4, respectively. The triply bridging coordination of C(1)O(1) on the tilted triangular face of the Pd(3) and two Pd(7) atoms results in the O(1) atom lying on the pseudo fivefold Pt(0)−Pd(1)−Pd(3) axis; this superimposed position of the O(1) atom on top of Pd(3) is not apparent from Figure 4, because the pseudo fivefold axis passing through the Pd(3) and O(1) atoms is not perpendicular to the viewer. The C(3)O(3) carbonyl is additionally disordered with respect to the above cited mirror plane; only one disordered position is shown in Figure 4.

The two types of *intershell* CO ligation found in **1**: namely, (a) C(1)O(1) connecting exclusively two *inner shells*; and (b) the other three independent COs connecting the *outer shell* with the adjacent inner shell are consistent with the two-band solid-state IR spectrum of **1** (*vide infra*).

Synthesis. Black crystals of **1** were reproducibly prepared in small yields (<5−10%) from the short-time reaction of $Pd_{10}(CO)_{12}(PPh_3)_6$[33] (**3**) with 3 equiv of $Pt(CO)_2(PPh_3)_2$[34] (**4**) in THF under N_2 at moderately elevated temperature followed by crystallization in the presence of acetone also under N_2.

$$Pd_{10}(CO)_{12}(PPh_3)_6\ (\mathbf{3}) + Pt(CO)_2(PPh_3)_2\ (\mathbf{4}) \rightarrow Pd_{157}Pt_8(CO)_{72}(PPh_3)_{20}\ (\mathbf{1}) + \ldots \quad (1)$$

It should be noted that crystallizations *under CO* from solutions obtained from similar reactions gave quantitatively heterometallic butterfly clusters, $Pd_nPt_m(CO)_5(PPh_3)_4$, $n + m = 4$.[35]

Generally, metal-core enlargement of palladium carbonyl/phosphine clusters $Pd_n(CO)_xL_y$, $L = PR_3$ occurs in the presence of reagents that promote the deligation of the metal-core by their binding the ligands: for example, via oxidation with O_2, H_2O_2, or Me_3NO, via protonation with CF_3CO_2H, CH_3CO_2H, HCO_2H, etc., or via complexation with $Pd(OAc)_2$, $(PhCN)_2PdCl_2$, Pd_2dba_3, $Co_2(CO)_8$, etc. Although spontaneous palladium-core enlargement is known,[3i] the condition of ligand-deficiency certainly favors the growth of larger-sized palladium carbonyl/phosphine clusters. In this connection, the generation of the giant M_{165} cluster (**1**) by reaction (1) is notable: namely, the coordinatively saturated reagent **4** supplies the reaction medium with extra PPh_3 instead of eliminating these ligands from **3** (*vide supra*). In fact, in all large $Pd_n(CO)_xL_y$ clusters which have at least one interstitial metal atom as well as in all known heterometallic $Pd_nPt_m(CO)_xL_y$ clusters, the number of metal atoms generally exceeds by at least twice the number of phosphine L ligands [i.e., $y/(n + m) < 0.5$]; in contrast, the addition to **3** of 3 equiv of **4** results in the number of potentially available PPh_3 ligands being larger than the total number of metal atoms [i.e., $y/(n + m) > 1$]. Furthermore, reaction (1) must involve complete cleavage of the relatively strong Pt−CO and Pt−PPh_3 bonds (versus those of Pd) in precursor **4** in order to furnish interstitial Pt atoms in **1**. Whether or not the presence of Pt atoms is necessary for the formation of the 165-atom cluster is still unclear; extensive efforts will continue to be made to obtain the Pd_{165} analogue of **1**. The fact that the

(33) Mednikov, E. G.; Eremenko, N. K.; Gubin, S. P. *Koordin. Khim.* (*Sov. J. Coord. Chem.*) **1984**, *10*, 711.
(34) Giannoccaro, P.; Sacco, A.; Vasapollo, G. *Inorg. Chim. Acta* **1979**, *37*, L455.
(35) Mednikov, E. G.; Dahl, L. F., unpublished research.

radial metal−metal bonding between the central Pt atom and the 12 icosahedral cage atoms in shell 1 of **1** would be stronger than that between a central Pd atom and its 12 icosahedral Pd atoms provides a partial rationalization for the nonexistence (as yet) of the Pd_{165} analogue of **1**.

Future plans include a systematic exploration of related reactions including ones involving changes in solvent polarity and pH.

Spectroscopic (IR, NMR) Analysis. A solid-state IR spectrum of **1** in nujol exhibited one strong broad band at 1878 cm^{-1} that overlapped with a middle-weak, shoulder-type band at 1779 cm^{-1}, and a separate middle-weak band at 1701 cm^{-1} which was readily attributed to solvated acetone molecules. These IR bands are consistent with the crystal structure containing only bridging carbonyls as well as solvated acetone molecules.

Because of the extremely low solubility of the crystals of **1** in CD_2Cl_2, both $^{31}P\{^1H\}$ and ^1H NMR spectra were acquired over large number of scans (namely, 27 100 and 700 scans, respectively). However, the $^{31}P\{^1H\}$ NMR spectrum of **1** did not afford interpretable information on chemical shift(s); this nondetection could have been caused by its possible decomposition under *partial* dissolution of crystals (50 min of sonication) and under the long duration of data collection (∼14 h). A ^1H NMR spectrum of **1** displayed broad proton peaks at 7.2 ppm (m) characteristic of phenyl substituents and methyl protons of acetone molecules at 2.12 ppm (s); the observed intensity ratio of 300/47 is reasonably close to the crystallographically defined ratio of 300/36. This ^1H NMR spectrum also revealed two characteristic patterns of $-C\mathbf{H}_2$-O$-C\mathbf{H}_2-$ and $C-C\mathbf{H}_2-C\mathbf{H}_2-C$ protons for THF molecules at 3.68 ppm (m) and 1.82 ppm (m), respectively, with equivalent intensities of 20 relative to that of the phenyl protons; these spectral data correspond to an estimated number of ∼10 solvated THF molecules per unit cell. The ^1H NMR spectrum also indicated the presence of solvated hexane molecules in **1**, but estimation of a reliable number was essentially hindered by signals from impurities contained in CD_2Cl_2. In fact, the control ^1H spectrum of CD_2Cl_2 displayed *the same* chemical shifts characteristic of hexane at $\delta_1 = 1.26$ ppm (typical for $-C\mathbf{H}_2-$) and $\delta_2 = 0.88$ ppm (typical for $-C\mathbf{H}_3$) with an intensity ratio of $\delta_1/\delta_2 = 2/1$. However, upon the dissolving of **1** in CD_2Cl_2, we observed an approximate 2.5 time-increment in the intensities of these signals relative to residual protons of CD_2Cl_2 (viz., $CHDCl_2$) at 5.32 ppm.

Conclusions

The 165 metal-core of **1** is the largest crystallographically characterized discrete metal cluster with direct metal−metal bonding. Complementary to the "filled" four-shell description, the metal-core of **1** can also be considered in terms of a pseudo-I_h Pt-centered six-shell ν_1 polyhedral system comprised of concentric coordination spheres with metal atoms within each shell located at the same radial distance from central Pt atom. In this case, the 42-atom ν_2 shell 2 is classified as a separate 30-atom ν_1 icosidodecahedral shell and a 12-atom ν_1 icosahedral shell, while the 50-atom ν_2 shell 4 is viewed as the composite of a 30-atom ν_1 icosidodecahedral shell and a 20-atom ν_1 pentagonal dodecahedral shell. The total six-shell ν_1 polyhedralarrangement, denoted as $Pt@M_{12}@M_{30}@M_{12}@M_{60}@M_{30}@M_{20}$, is presented in Figure 5. The diameter of the entire spheroidal-shaped metal core between two centrosymmetrically opposite vertices of the pentagonal dodecahedron is 1.73 nm.

Structural *similarities* between **1** and **2** are: (1) both metal-core geometries possess pseudo-icosahedral I_h symmetry; (2) corresponding shells 1 and 2 are virtually identical and corresponding shells 3 similar; (3) 30 square-capped Pd atoms in **2** correspond to the 30 middle-edge pentagonal-sided Pd atoms in **1** that are each weakly connected (3.1 Å) to two 20 triangular-capped Pd vertices of the fourth ν_2 pentagonal dodecahedral shell. Completely surprising structural *dissimilarities* between **1** and **2** are: (1) to date, **1** is only reproducibly isolated as a heterometallic Pd−Pt cluster with a central Pt instead of Pd atom; (2) the 50 atoms comprising the outer fourth ν_2 pentagonal dodecahedral shell in **1** are *less* than the 60 atoms of the inner third shell in **1**, in contradistinction to shell-by-shell growth processes in all other known shell-based structures; (3) the 10 fewer PR_3 ligands in **1** necessitate larger bulky PPh_3 ligands to protect the Pd−Pt core-geometry; (4) the 72 CO ligands consist of six bridging COs within each of the 12 pentagons in shell 4 that are coordinated to *intershell* metal atoms—namely, the central CO links shells 2 and 3, and the outer five COs each link shells 3 and 4. It is apparent that both the *intershell*-connecting COs and bulky PPh_3 ligands in **1** are essential in the formation and stabilization of this remarkable cluster, whereas in **2** smaller PEt_3 ligands are likewise required to sterically accommodate its 30 capping Pd atoms.

The observed stereochemistry of **1** and its method of preparation clearly indicate that: (1) the long-term assumption about the necessity of using relatively small ligands with minimal steric effects in order to form large clusters,[36] (in the case of palladium carbonyl/phosphine clusters such ligands are PMe_3, PEt_3, and PMe_2Ph), is *not without exception*; (2) in a (*dimple-ball*)-shaped multi-shell cluster such as **1**, ligand-penetration to give *intershell* COs that stabilize the cluster-formation may occur; (3) the *coordinatively saturated* zerovalent Pt(0) compound, $Pt(CO)_2(PPh_3)_2$, can be reacted with an appropriate zerovalent Pd(0) precursor, $Pd_{10}(CO)_{12}(PPh_3)_6$, to generate large Pt/Pd heterometallic carbonyl/phosphine clusters, thereby avoiding conventional but more complicated and often less controllable redox reactions;[37] and (4) platinum atoms obtained from complete deligation of such a precursor can serve as centers of cluster growth.

Experimental Section

General Comments. Reactions were carried out via standard Schlenk techniques on a preparative vacuum line under nitrogen atmosphere. Solvents were deoxygenated by the purging of N_2 through them for at least 20 min at room-temperature prior to their use. $Pd_{10}(CO)_{12}(PPh_3)_6$[33] and $Pt(CO)_2(PPh_3)_2$[34] were prepared in accordance with published methods. Infrared spectra were recorded on a Mattson Polaris FT-IR spectrometer; nujol mulls were prepared under nitrogen. Room-temperature $^{31}P\{^1H\}$ NMR (121.4 MHz) and ^1H (299.9 MHz) spectra of **1** in CD_2Cl_2 solution were obtained under a N_2 atmosphere on a Bruker AC-300 spectrometer and referenced to 85% H_3PO_4 in D_2O as

(36) Chini, P. *J. Organomet. Chem.* **1980**, *200*, 37.
(37) (a) Mononuclear *coordinatively saturated* $Pd(PPh_3)_4$, which earlier was directly converted into $Pd_{10}(CO)_{12}(PPh_3)_6$,[37b] was recently used for laser-induced generation of palladium nanoparticles;[37c] in both conversions, metal aggregation was achieved without change in metal oxidation state. (b) Mednikov, E. G.; Eremenko, N. K. *Izv. Acad. Nauk SSSR. Ser. Khim.* **1984**, 2781. [*Bull. Acad. Sc. USSR, Div. Chem. Sc.* (Engl. Transl.) **1984**, *33*, 2547]. (c) Ye, E.; Tan, H.; Li, S.; Fan, W. Y. *Angew. Chem., Int. Ed.* **2006**, *45*, 1120.

an external phosphorus standard and to residual protons of CD_2Cl_2 as an internal hydrogen standard, respectively. X-Ray Pd/Pt microanalyses were performed with Pt and Pd metals as standards on the wavelength-dispersive spectrometer (WDS) Cameca SX51 and without standards on the scanning electron microscope LEO 1530 with an energy-dispersive detector. Variable-temperature magnetic susceptibility data were obtained on a Quantum Design MPMS-XL SQUID magnetometer.

Preparation of (μ_{12}-Pt)$Pd_{164-x}Pt_x(CO)_{72}(PPh_3)_{20}$ ($x \approx 7$), 1, and Spectral/Magnetic Data. In a typical reaction, a solution of $Pd_{10}(CO)_{12}(PPh_3)_6$ (0.200 g, 0.0672 mmol) and $Pt(CO)_2(PPh_3)_2$ (0.1565 g, 0.2018 mmol) in THF (8 mL) was stirred for 30 min under N_2 at 65 °C. The formed brown solution was evaporated to ~3 mL under N_2 flow, filtered, and then crystallized in the presence of vapors from mixture of acetone/hexane (4/1) under N_2. At the initial stage of crystallization (one week), multiply interpenetrating black crystals of hexagonal morphology were formed that produced extremely poor X-ray diffraction patterns. Nevertheless, prolonged crystallization afforded ~8−10 mg of well-shaped, block-like black crystals of (μ_{12}-Pt)$Pd_{164-x}Pt_x(CO)_{72}(PPh_3)_{20}$·$6Me_2CO$, $x \approx 7$ (**1**) that were manually separated from ~15 mg of the hexagonal-like black plates. This method was found to be reproducible in affording crystals of **1** with the same characteristic morphology, unit-cell parameters, and infrared spectra. Spectral data for **1**: IR ν_{CO} (cm^{-1}): 1878 (s), 1779 (m-w, sh), 1701 (m-w). ^1H NMR (300 MHz, CD_2Cl_2, rt) $\delta = 7.2$ (m, 300 H, C_6H_5), 3.68 (m, CH_2OCH_2, THF), 2.12 (s, 36 H, acetone), 1.82 (m, CC_2H_4C, THF). $^{31}P\{^1H\}$ NMR (121 MHz, CD_2Cl_2, rt, 85% *ortho*-H_3PO_4); no noticeable/reliable signals were obtained. Mass-normalized magnetization measurements performed (by M.J.) on a SQUID magnetometer revealed a single-crystal sample of **1** to be diamagnetic with a constant magnetic moment of -1.2×10^{-3} emu/g over the entire temperature range of 10−300 K. The observed diamagnetism is especially informative in light of the structure of **1** containing both encapsulated Pd and Pt atoms.

X-Ray Crystallographic Determination. A block-shaped crystal of size $0.58 \times 0.52 \times 0.45$ mm^3 was selected for data collection. Intensity data were collected over an entire reciprocal lattice sphere at 100(2) K via a Bruker SMART CCD-1000 area-detector system mounted on a Bruker *P*4 diffractometer with graphite-monochromated Mo Kα radiation from a standard sealed-tube generator. A multiscan absorption correction (SADABS) was applied [μ(Mo−Kα) = 5.484 mm^{-1}; max/min transmission, 0.192/0.143]. The entire crystal structure was obtained by combined use of direct methods/difference Fourier syntheses together with least-squares refinement (based on F^2) that was performed with SHELXTL.[38] Each of the two clusters (**1**) in the unit cell, which are symmetry-related by the body-centered (I) cubic space group, possesses $2/m\bar{3}$ (T_h) site symmetry. Twelve equivalent solvated disordered acetone molecules were additionally found in the unit cell. Solvated THF/hexane molecules (detected from a ^1H NMR spectrum) were not resolved or modeled due to their possible partial occupancy and/or presumed multiple crystal disorders under $I2/m\bar{3}$ symmetry, which gave rise to the resulting residual electron density peaks on the final difference Fourier map being weak and uninterpretable.

$PtPd_{164-x}Pt_x(CO)_{72}(PPh_3)_{20}$ ($x \approx 7$)·$6CH_3C(O)CH_3$: M = 25879.47, cubic; space group $I2/m\bar{3}$; $a = b = c = 32.862(1)$ Å, $\alpha = \beta = \gamma = 90°$, $V = 35486.4(15)$ $Å^3$; $Z = 2$, $\rho_{calcd} = 2.420$ Mg/m^3. A sphere of 39 960 data was collected via 0.3ω scans over a 2θ range of 3.92−42.84° with crystal-detector distance at 73.46 mm. Refinement (152 parameters; 58 restraints) on 3200 independent merged reflections (R(int) = 0.0575) converged at $\omega R_2(F^2) = 0.303$ with $R_1(F) = 0.111$ for $I > 2\sigma(I)$; GOF(on F^2) = 1.37; max/min residual electron density 2.52/−2.19 e·$Å^{-3}$.

The crystallographically independent part of **1** consists of its central Pt atom, 7 site-disordered Pd/Pt atoms in shells 1−3, four Pd atoms in shell 4, two phosphorus atoms, one whole-weighted $C_6H_5(1)$ ring and three-half-weighted $C_6H_5(2)$, $C_6H_5(3)$, and $C_6H_5(4)$ rings that are randomly disordered between two orientations, and four bridging carbonyl ligands, of which one, C(3)O(3), is randomly disordered between two orientations. All metal and phosphorus atoms were refined anisotropically; identical atomic coordinates were used for the 7 independent compositionally disordered Pt/Pd positions.

The carbonyl carbon and oxygen atoms and phenyl carbon atoms as well as the four non-hydrogen atoms of the independent, crystal-disordered acetone molecule were refined isotropically. The four phenyl rings were modeled as rigid groups. No hydrogen atoms were generated.

Individual isotropic displacement parameters were utilized for the six carbon atoms of the whole-weighted $C_6H_5(1)$ ring attached to the P(1) atom lying on the crystallographic threefold axis; identical isotropic displacement parameters were used for the six carbon atoms of each of the other half-weighted phenyl rings that were disordered by the mirror passing through the attached P(2) atom. This disorder corresponds to two pseudo threefold-related orientations of the three P(2)-attached phenyl rings.

Identical carbon and oxygen isotropic displacement parameters were used for each of the half-weighted C(3)O(3) and full-weighted C(4)O(4) groups; the C(3)O(3) ligand is disordered over two sites by the crystallographic mirror passing through the Pd(3), Pd(6), Pd(9), Pd(11) atoms. (Figure 4 shows only one disordered orientation). Distance restraints were applied to all C−O and P−C connectivities.

The atomic parameters in Table S1 are consistent with the four non-hydrogen atoms (*viz*., O(40), C(40), $H_3C(41)$, $H_3C(42)$) of the independent acetone molecule in the unit cell possessing an orientational disorder (i.e., one in which the carbonyl carbon atom, C(40), of one-half-weighted orientation is nearly superimposed on the methyl C(42) atom of the other half-weighted orientation). This table also reveals that the atomic parameters for each of these four-half-weighted acetone atoms closely correspond to *x*, 0, 1/2 which belongs to set 12e of site symmetry *mm*2 in the $I2/m\bar{3}$ space group.[39] This indicates that the 12 solvated acetone molecules are additionally slightly disordered within 12 equiv cavities per unit cell defined by the body-centered cubic packing of the clusters. It is tempting to speculate that solvated THF/hexane molecules occupy 12 equiv cavities corresponding to set 12d of site symmetry *mm*2,[39] in spite of there being no crystallographic evidence for this possibility.

Nevertheless, the resolution from difference Fourier syntheses of the four independent carbonyl groups and four independent phenyl rings enabled the non-hydrogen ligand composition to be determined for this extraordinary cluster. Likewise, the least-squares analysis of disordered Pt_xPd_{1-x} sites for the central atom and seven independent positions in shells 1−3 played an essential role in establishing the distribution of Pt/Pd atoms in **1**; the resulting total number of ~8 Pt atoms was fortuitously found to be in agreement with that obtained from an X-ray Pt/Pd microanalysis of single crystals.

Figure 6 displays a typical CCD area-detector frame which reveals high diffuse scattering attributed to "defect" crystal packing. Analogous high-diffuse scattering was previously encountered in the crystal structure determinations of both the Pd_{145} cluster (**2**)[3r] and $Pd_{66}(CO)_{45}(PEt_3)_{16}$.[3o] Although this non-Bragg scattering imposes a considerable systematic error in the collected intensity data, the successful structural determination of **1** is ascribed to the collection of a full sphere of low-temperature area-detector CCD X-ray data. This collection of many equivalent reflections under cubic $2/m\bar{3}$ (T_h) symmetry gave rise to a reasonably reliable empirical (multiscan) absorption correction (SADABS), as reflected by the low R_{inter} value of 0.0575 for the merging of 39 960 reflections into approximately 3400 independent reflections (of

(38) (a) Sheldrick, G.: all crystallographic software and sources of the scattering factors are contained in the SHELXTL (version 6.14 (2000−2003)) program library, Bruker Analytical X-Ray Systems, Madison, WI. (b) Müller, P.; Herbst-Irmer, R.; Spek, A. L.; Schneider, T. R.; Sawaya, M. R. *Crystal Structure Refinement: A Crystallographer's Guide to SHELXL*; Müller, P., Ed.; International Union of Crystallography: Oxford University Press, 2006.

(39) International Tables for Crystallography. Space Group Symmetry; Hahn, T., Ed.; D. Reidel Publ. Co.: Boston, 1983; Vol. A, pp 618−619.

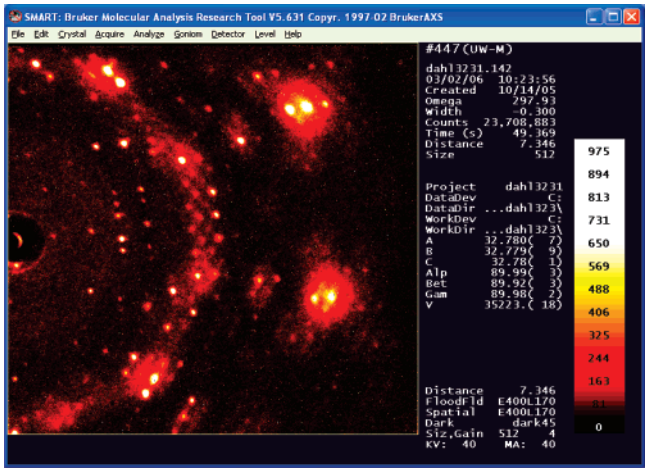

Figure 6. Typical CCD area-detector frame showing diffraction pattern (at 100 K) of nanosized (μ_{12}-Pt)$Pd_{164-x}Pt_x(CO)_{72}(PPh_3)_{20}$ ($x \approx 7$), **1**, with high diffuse scattering attributed to "defect" crystal packing.

which ~200 were then deleted on the basis of an observed $|F(hkl)|_o$ being at least 10 times that of the calculated $|F(hkl)|_c$, no doubt due to the high-diffuse scattering background); it also provided an excellent data-to-parameter ratio of ~20/1 that subsequently led to the elucidation of the molecular structure. A structural CIF/PLATON test carried out by the http://journals.iucr.org/services/cif/checking/checkform.html service is in accordance with our crystal structure determination.

The body-centered unit cell of the crystal structure of **1** contains roughly 12 000 Å^3 of accessible voids, which hypothetically could be filled by ~60 solvated acetone/THF/hexane molecules used for the crystallization of **1**. Formation of such enormous voids in the crystal structure of **1** is imposed by two geometrical factors: (a) large spherical molecules of **1** *per se*, of an estimated 2.7 nm diameter (between centrosymmetrically related outermost carbon atoms of the phenyl rings); and (b) a space-filling of 68% for two spheres in a body-centered cubic cell. However, the number of crystallographically found solvated acetone molecules and ^{1}H NMR-estimated THF molecules are only 12 and 10, respectively. We assume that the large voids may also contain solvated hexane molecules, as suggested by the ^{1}H NMR data (*vide supra*). CCDC reference number is 649053.

Acknowledgment. This research was supported by the National Science Foundation. The CCD area detector system was purchased, in part, from NSF grant, CHE-9310428. The Bruker AC-300 NMR spectrometer was purchased, in part, by funds from NSF CHE-9208963 and NIH SIO RR 08389-01. Color figures were prepared with Crystal Maker, Interactive Crystallography Software [David C. Palmer, Begbroke Park, Bldg 5, Sandy Lake, Yarnton OX51PF (UK)]. We are especially grateful for X-ray Pt/Pd microanalysis to Dr. John Fournelle (Department Geology & Geophysics, UW-Madison) and to Dr. Richard Noll (Engineering Experiment Station, UW-Madison) and for crystallographic advice to Dr. Ilia Guzei (UW-Madison). Dedicated to Professor Dr. Heinrich Vahrenkamp.

Supporting Information Available: Structural analysis and Table S1, which presents the atomic coordinates, number of symmetry-equivalent positions, crystallographic site symmetry, equivalent isotropic displacement parameters for the independent anisotropically refined metal and phosphorus atoms, and isotropic displacement parameters for the carbon and oxygen atoms in the crystal structure. This material is available free of charge via the Internet at http://pubs.acs.org.

JA073945Q